



## **Ion-precursor and ion-dose dependent anti-galvanic reduction**

Journal:	<i>ChemComm</i>
Manuscript ID:	CC-COM-04-2015-003267.R1
Article Type:	Communication
Date Submitted by the Author:	31-May-2015
Complete List of Authors:	Tian, Shubo; Institute of Solid State Physics, Yao, Chuanhao; Institute of Solid State Physics, Liao, Lingwen; Institute of Solid State Physics, Xia, Nan; Institute of Solid State Physics, Wu, Zhikun; Institute of Solid State Physics,



Journal Name

COMMUNICATION

## Ion-precursor and ion-dose dependent anti-galvanic reduction

 Shubo Tian,<sup>‡a</sup> Chuanhao Yao,<sup>‡a</sup> Lingwen Liao,<sup>a</sup> Nan Xia<sup>a</sup> and Zhikun Wu<sup>\*a</sup>

 Received 00th January 20xx,  
Accepted 00th January 20xx

DOI: 10.1039/x0xx00000x

www.rsc.org/

**Controlling alloy nanoparticles with atomically monodispersity is challenging, and the recently revealed anti-galvanic reduction (AGR) provides a unique solution to this challenge. Herein we demonstrate that AGR is ion-precursor and ion-dose dependent, which offers novel strategies to tune the compositions, structures and properties of nanoparticles by varying the ion-precursor and ion-dose in AGR reaction.**

Bimetal nanoparticles attract extensive interests for long lasting years due to their intriguing properties which are not exhibited by mono-metal nanoparticles.<sup>1–6</sup> To insightfully understand the properties of bimetal nanoparticles, controlling bimetal nanoparticles with atomic monodispersity is of prime importance. Enormous efforts have been put into the achievement of this aim.<sup>4,7–15</sup> Popular method for the synthesis of atomically precise bimetal nanoparticles is the synchro-synthesis method which was once utilized for the synthesis of Au<sub>24</sub>Pd(SR)<sub>18</sub> (SR=SC<sub>12</sub>H<sub>25</sub>, SC<sub>2</sub>H<sub>4</sub>Ph, S(CH<sub>2</sub>CH<sub>2</sub>O)<sub>5</sub>CH<sub>3</sub>),<sup>16,17</sup> Au<sub>24</sub>Pt(SR)<sub>18</sub> (SR=SC<sub>2</sub>H<sub>4</sub>Ph),<sup>18</sup> Au<sub>25–x</sub>Cu<sub>x</sub>(SR)<sub>18</sub> (SR=SeC<sub>8</sub>H<sub>17</sub>),<sup>19</sup> Au<sub>25–x</sub>Ag<sub>x</sub>(SR)<sub>18</sub> (SR=SC<sub>12</sub>H<sub>25</sub>, SC<sub>2</sub>H<sub>4</sub>Ph, SC<sub>n</sub>H<sub>2n</sub>COOH),<sup>8,13,20,21</sup> Au<sub>38–x</sub>Ag<sub>x</sub>(SR)<sub>18</sub> (SR=SC<sub>2</sub>H<sub>4</sub>Ph),<sup>22</sup> Au<sub>36</sub>Pd<sub>2</sub>(SR)<sub>24</sub> (SR=SC<sub>2</sub>H<sub>4</sub>Ph),<sup>23</sup> etc., however, only few bimetal nanoparticles with atomic monodispersity were obtained by this method;<sup>16–18</sup> galvanic reduction (GR) is another well-known method to engineer the compositions, structures and properties of nanoparticles.<sup>7,24–35</sup> Unfortunately, no atomically monodisperse bimetal nanoparticles (AMBN) were reported so far by GR. Overall, the synthesis of AMBN is still challenging. Fortunately, the recently revealed anti-galvanic reduction (AGR) provides a unique strategy to access AMBN<sup>36–42</sup> and very recently atomically mono-disperse Au<sub>25</sub>Ag<sub>2</sub>(PET)<sub>18</sub>(PET=SC<sub>2</sub>H<sub>4</sub>Ph)<sup>42</sup> was successfully synthesized in two minutes, high yield (89%) and gram scale by this unusual method. Interestingly, it is shown when silver ion is replaced by Cu<sup>2+</sup> in the reaction with anion Au<sub>25</sub>(PET)<sub>18</sub>, Au<sub>44</sub>(PET)<sub>32</sub><sup>41</sup> instead of the Au/Cu bimetal nanoparticles can be obtained, which indicates that the AGR is dependent of the ion species and not only limited for the synthesis of alloy nanoparticles. One possible reason is that

different ion species are of various reduction potential and coordination nature. A question naturally arising is whether the AGR is dependent of the ion precursors which influence the ion (or its reduction state) release. To unravel this question, we test the reaction between anion Au<sub>25</sub>(PET)<sub>18</sub><sup>–</sup>(N(C<sub>8</sub>H<sub>17</sub>)<sub>4</sub>)<sup>+</sup> as the counter ion) and four different silver ion precursors respectively. Indeed, the experimental results demonstrate that AGR is ion-precursor dependent, and additional experiments reveal that AGR is also ion-dose dependent. Below we will present more details and discussion.

EDTA, DTZ and PET are some common chelants for metal ions, and they exhibit different chelating nature and ability to silver ions/atoms (i.e. Ag-EDTA, Ag-PET and Ag-DTZ complexes have distinctly different releasing ability to silver ions/atoms), so Ag-EDTA, Ag-PET and Ag-DTZ complexes plus AgNO<sub>3</sub> were chosen as silver ion precursors due to that they exhibit various releasing ability of silver ions/atoms (EDTA: ethylenediamine tetraacetic acid disodium salt; PET: 2-Phenylethanethiol; DTZ: Dithizone). First, Ag-EDTA, Ag-PET and Ag-DTZ complexes were prepared by simply mixing the according ligand with AgNO<sub>3</sub>, then they together with AgNO<sub>3</sub> were added into the toluene solution of anion Au<sub>25</sub>(PET)<sub>18</sub>, respectively (for convenience of comparison, the Ag/Au<sub>25</sub>(PET)<sub>18</sub> molar ratio in all cases are 2:1). One hour later, the four reactions were stopped by the addition of excessive petroleum ether, the as-

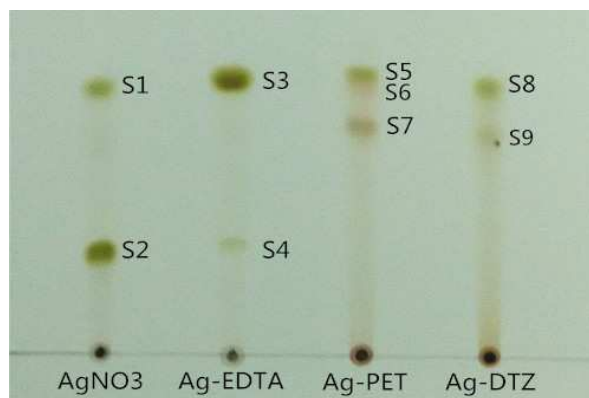


Fig. 1 Photograph of the TLC plate. From left to right, AgNO<sub>3</sub>, Ag-EDTA, Ag-PET and Ag-DTZ were used as the precursor.

<sup>a</sup> Key Laboratory of Materials Physics, Anhui Key Laboratory of Nanomaterials and Nanostructures, Institute of Solid State Physics, Chinese Academy of Sciences, Hefei 230031, China. E-mail: [zkwu@issp.ac.cn](mailto:zkwu@issp.ac.cn)

Electronic Supplementary Information (ESI) available: [detailed information about the synthesis, Characterizations and MALDI-TOF-MS spectra of S6, S7 and S9]. See DOI: 10.1039/x0xx00000x

‡ S.T. and C.Y. contributed equally to this work.



Journal Name

## COMMUNICATION

Tab. 1 Summary of the assignments of TLC spots.

Precursor	2eq. AgNO <sub>3</sub>	2eq. Ag-EDTA	2eq. Ag-PET	2eq. Ag-DTZ	0.5eq. Ag-DTZ	1eq. Ag-DTZ
	Au <sub>25-x</sub> Ag <sub>x</sub> (PET) <sub>18</sub> <sup>0</sup> , (S1; x=0,1)	Au <sub>25</sub> (PET) <sub>18</sub> <sup>0</sup> , (S3)	Au <sub>25</sub> (PET) <sub>18</sub> <sup>0</sup> , (S5)	Au <sub>25-x</sub> Ag <sub>x</sub> (PET) <sub>18</sub> <sup>0</sup> , (S8; x=0,1,2)	Au <sub>25-x</sub> Ag <sub>x</sub> (PET) <sub>18</sub> <sup>0</sup> , (S10; x=0,1)	Au <sub>25-x</sub> Ag <sub>x</sub> (PET) <sub>18</sub> <sup>0</sup> , (S12; x=0,1,2)
	Au <sub>25</sub> Ag <sub>2</sub> (PET) <sub>18</sub> <sup>0</sup> , (S2)	Au <sub>25</sub> Ag <sub>2</sub> (PET) <sub>18</sub> <sup>0</sup> , (S4)	unknown (S6,S7)	unknown (S9)	Au <sub>25</sub> Ag <sub>2</sub> (PET) <sub>18</sub> <sup>0</sup> , (S11)	Au <sub>25</sub> Ag <sub>2</sub> (PET) <sub>18</sub> <sup>0</sup> , (S13)

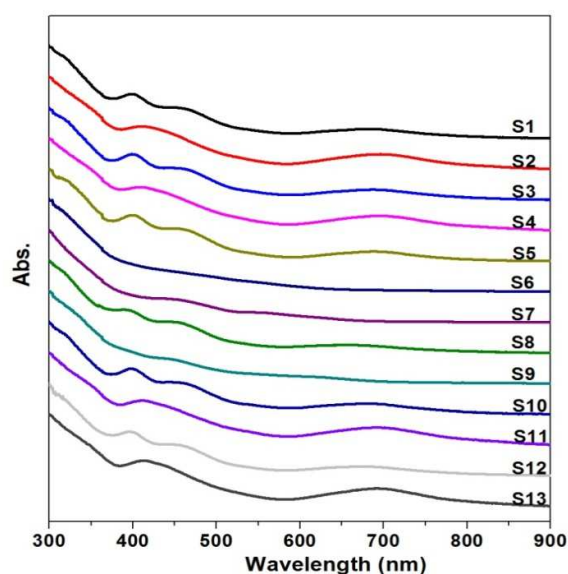


Fig. 2 UV/Vis/NIR spectra of S1-13.

obtained precipitates were collected and thoroughly washed with methanol, then used for thin-layer chromatography (TLC) analyses,<sup>42,43</sup> (CH<sub>2</sub>Cl<sub>2</sub>/petroleum ether as developing solvent). To be noted, the whole process (including reaction, post-treatment and analysis by TLC) was facilitated conducted in room temperature without the avoiding of light and air. Interestingly, TLC shows distinct difference of the product components in the four cases (see Figure 1, from left to right, AgNO<sub>3</sub>, Ag-EDTA, Ag-PET and Ag-DTZ were used as the silver ion precursor, respectively). For convenience, the spots in the TLC plate were sequentially numbered as S1-9 (see Figure 1). It is clear that the products contain minor S1 and major S2 when AgNO<sub>3</sub> was used as the silver-ion resource; when Ag-EDTA was used as the silver ion precursor, the products contain dominant S3 and trace of S4; In the case of Ag-PET, the products are a little complex and there are two comparable components S5 and S7, together with one minor component S6; In the case of Ag-DTZ, one distinct component S8 and one vague component S9 were found in the TLC plate. Preliminarily judged by the TLC, S3 and S5 may be the same compound since that they show same mobility and colour in the plate. Similarly, S2 and S4 may be identical. To identify the

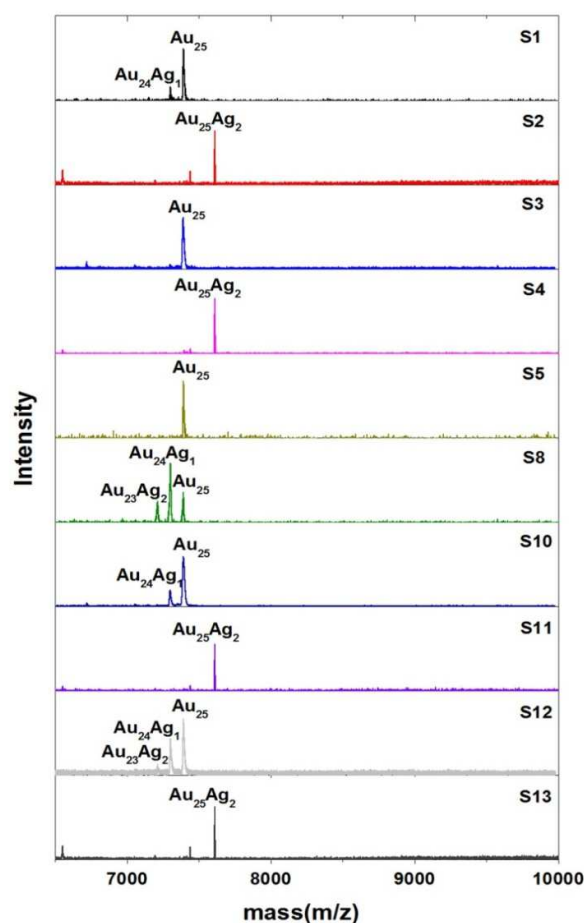


Fig. 3 MALDI-TOF-MS spectra of S1-5, S8 and S10-13. The mass spectra of S1, 3, 5, 8, 10, 12 were acquired in the negative ionization mode, while the left spectra were recorded in the positive ionization mode.

components, all of them (S1-9) were isolated from the preparative thin-layer chromatography (PTLC) plate and further analyzed by UV/Vis/NIR spectrometry, together with matrix-assisted laser desorption/ionization time of flight mass spectrometry (MALDI-TOF-MS). UV/Vis/NIR spectra reveal that both S3 and S5 are neutral

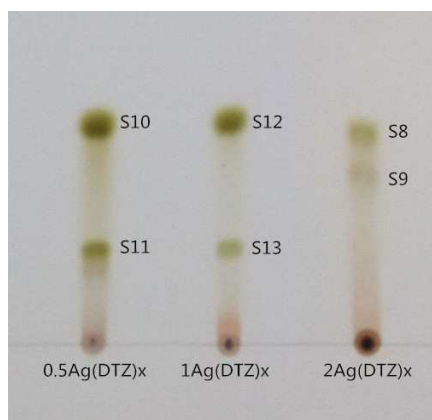


Fig. 4. Photograph of the TLC plate. From left to right, 0.5eq Ag-DTZ, 1eq Ag-DTZ and 2eq Ag-DTZ were used in the AGR reaction.

$Au_{25}(PET)_{18}$ <sup>44,45</sup> (see Figure 2), which was further confirmed by MALDI-TOF-MS (see Figure 3). UV/Vis/NIR spectra, together with MALDI-TOF-MS reveal that S2 and S4 are indeed identical  $Au_{25}Ag_2(PET)_{18}$ , an alloy nanoparticles which we reported very recently.<sup>42</sup> Surprisingly, S1 is identified to be a mixture of  $Au_{25}(PET)_{18}$  (major) and  $Au_{24}Ag(PET)_{18}$  (minor) by MALDI-TOF-MS (Figure 3), and S8 concurrently contains  $Au_{25}(PET)_{18}$  (minor),  $Au_{24}Ag(PET)_{18}$  (major) and  $Au_{23}Ag_2(PET)_{18}$  (minor), which indicate MALDI-TOF-MS is a better way to monitor the purity of such samples than TLC and UV/Vis/NIR spectrum. Unfortunately, the fragmentation in MALDI-TOF-MS retards the rational assignments of S6, S7 and S9 (Fig S1-3), and further efforts are underway to grow high qualified single crystals and they are thereafter not discussed in this work. A summary of the assignments of TLC spots is shown in table 1, which clearly demonstrates that AGR is strongly dependent of ion-precursor. Interestingly, the starting spots also show difference between anion  $Au_{25}(PET)_{18}$  and ion precursors demonstrated by UV/Vis/NIR and MALDI-TOF-MS (see Figure S4-8): Lumps centered at  $M/Z \sim 11K$  and  $\sim 8.9K$  in mass spectra (Fig. S5 and S7) indicate the forming of some big nanoclusters (compared with  $Au_{25}(PET)_{18}$ ) when  $AgNO_3$  and Ag-PET employed as the ion precursors, the  $M/Z \sim 6030$  peak in Fig. S6 indicates the production of small immobile nanoclusters when Ag-EDTA was used as the ion precursor, while the absence of peaks in the  $M/Z$  range from 2000 to 20000 in Fig. S8, together with the absence of plasma peak ( $\sim 520nm$ ) in Fig. S4 and the detection of Au by XPS (Fig. S9-10) indicates that  $Au_{25}(PET)_{18}$  partially discomposes to very small nanoclusters or complex in the case of Ag-DTZ. These results further demonstrate that the AGR is ion-precursor dependent. As proposed above, the ion (ion reduced state) release ability of the ion precursor may partly contribute to the ion-precursor dependence of AGR since that the main product is  $Au_{25}Ag_2(PET)_{18}$  when  $AgNO_3$  was used as the ion precursor, while in other three cases  $Au_{25}Ag_2(PET)_{18}$  is minor or even not found. Another consideration for the ion-precursor dependence is that the ligand may assist the atom replacement or recombination in AGR, which can be deduced from the fact that S8 mainly contains  $Au_{24}Ag(PET)_{18}$  (Ag-DTZ as the precursor) while S1 mainly contains neutral  $Au_{25}$  accompanied with minor  $Au_{24}Ag(PET)_{18}$  ( $AgNO_3$  as the ion precursor).

The dominance of  $Au_{24}Ag(PET)_{18}$  in S8 gives rise to a question: which is preferential in AGR, the simple oxidation of  $Au_{25}(PET)_{18}$  (from anion  $Au_{25}(PET)_{18}$  to neutral  $Au_{25}(PET)_{18}$ ) or the replacement of gold by silver (forming of  $Au_{25-x}Ag_x(PET)_{18}$ )? It is clear that the

former is preferential in the case when  $AgNO_3$  was used as the ion-precursor, however, it looks reverse in the case of Ag-DTZ (but a possible reason is the excess of silver precursor). To clarify this, we decrease the  $Ag/Au_{25}(PET)_{18}$  molar ratio to 1: 1 and 1: 0.5, and additionally test two reactions between anion  $Au_{25}(PET)_{18}$  and Ag-DTZ. It is revealed by MALDI-TOF-MS that in low dose of Ag-DTZ the dominant component of S10 and S12 (Figure 3,4) is neutral  $Au_{25}(PET)_{18}$  (in strong contrast to the case of S8, see Figure 1-4), and with the increase of Ag-DTZ dose the mono-replacement alloy nanoparticles ( $Au_{24}Ag(PET)_{18}$ ) increase and even the bi-replacement nanoparticles ( $Au_{23}Ag_2(PET)_{18}$ ) appear. The experimental results clearly show that the simple oxidation is preferential to the replacement in the reaction between anion  $Au_{25}(PET)_{18}$  and Ag-DTZ, too. Another interesting finding is the concurrently forming of  $Au_{25}Ag_2(PET)_{18}$  identified by TLC, UV/Vis/NIR spectrometry and MALDI-TOF-MS in low dose of Ag-DTZ (see figure 2-3). Taken together, these facts demonstrate that the AGR is also dose-dependent: the dose of Ag-DTZ can influence not only the relative content of neutral  $Au_{25}(PET)_{18}$  and doped  $Au_{25}(PET)_{18}$ , but also the product types. It's expected that novel nanoparticles (including alloy nanoparticles) can be synthesized by varying the ion-precursor and ion-dose in the AGR reaction, thus the advancement of AGR research in this work provides enormous and unusual opportunities of tuning the compositions, structures and properties of nanoparticles.

In summary, in this work we demonstrate that AGR is ion-precursor and ion-dose dependent, and we also reveal that the simple oxidation of anion  $Au_{25}(PET)_{18}$  is preferential to the concurrent replacement of gold in  $Au_{25}(PET)_{18}$  by silver in low dose of silver ion-precursor. The significance and novelty of this work lie in: It provides novel mechanism insight of AGR, and paves a way to tune the compositions, structures and properties of nanoparticles by varying the ion precursor and ion dose in AGR reaction.

This work was supported by National Basic Research Program of China (Grant No. 2013CB934302), the Natural Science Foundation of China (No. 21222301, 21171170), the Ministry of Human Resources and Social Security of China, the Innovative Program of Development Foundation of Hefei Center for Physical Science and Technology (2014FXCX002), the CAS/SAFEA International Partnership Program for Creative Research Teams and the "Hundred Talents Program" of the Chinese Academy of Sciences.

## Notes and references

- V. R. Stamenkovic, B. Fowler, B. S. Mun, G. Wang, P. N. Ross, C. A. Lucas and N. M. Markovic, *Science*, 2007, **315**, 493-497.
- B. Lim, M. Jiang, P. H. C. Camargo, E. C. Cho, J. Tao, X. Lu, Y. Zhu and Y. Xia, *Science*, 2009, **324**, 1302-1305.
- R. Subbaraman, D. Tripkovic, D. Strmcnik, K.-C. Chang, M. Uchimura, A. P. Paulikas, V. Stamenkovic and N. M. Markovic, *Science*, 2011, **334**, 1256-1260.
- H. Yang, Y. Wang, H. Huang, L. Gell, L. Lehtovaara, S. Malola, H. Hakkinen and N. Zheng, *Nat. Commun.*, 2013, **4**, 2422.
- C. Chen, Y. Kang, Z. Huo, Z. Zhu, W. Huang, H. L. Xin, J. D. Snyder, D. Li, J. A. Herron, M. Mavrikakis, M. Chi, K. L. More, Y.

- Li, N. M. Markovic, G. A. Somorjai, P. Yang and V. R. Stamenkovic, *Science*, 2014, **343**, 1339-1343.
- 6 G. Chen, Y. Zhao, G. Fu, P. N. Duchesne, L. Gu, Y. Zheng, X. Weng, M. Chen, P. Zhang, C.-W. Pao, J.-F. Lee and N. Zheng, *Science*, 2014, **344**, 495-499.
- 7 Y.-S. Shon, G. B. Dawson, M. Porter and R. W. Murray, *Langmuir*, 2002, **18**, 3880-3885.
- 8 Y. Negishi, T. Iwai and M. Ide, *Chem. Commun.*, 2010, **46**, 4713-4715.
- 9 Y. Negishi, K. Munakata, W. Ohgake and K. Nobusada, *J. Phys. Chem. Lett.*, 2012, **3**, 2209-2214.
- 10 T. Udayabhaskararao, Y. Sun, N. Goswami, S. K. Pal, K. Balasubramanian and T. Pradeep, *Angew. Chem., Int. Ed.*, 2012, **51**, 2155-2159.
- 11 H. Yang, Y. Wang, J. Lei, L. Shi, X. Wu, V. Maekinen, S. Lin, Z. Tang, J. He, H. Haekinen, L. Zheng and N. Zheng, *J. Am. Chem. Soc.*, 2013, **135**, 9568-9571.
- 12 N. Barrabes, B. Zhang and T. Buerger, *J. Am. Chem. Soc.*, 2014, **136**, 14361-14364.
- 13 C. Kumara, C. M. Aikens and A. Dass, *J. Phys. Chem. Lett.*, 2014, **5**, 461-466.
- 14 S. Wang, X. Meng, A. Das, T. Li, Y. Song, T. Cao, X. Zhu, M. Zhu and R. Jin, *Angew. Chem. Int. Ed.*, 2014, **53**, 2376-2380.
- 15 H. Yang, Y. Wang, J. Yan, X. Chen, X. Zhang, H. Hakkinen and N. Zheng, *J. Am. Chem. Soc.*, 2014, **136**, 7197-7200.
- 16 C. A. Fields-Zinna, M. C. Crowe, A. Dass, J. E. F. Weaver and R. W. Murray, *Langmuir*, 2009, **25**, 7704-7710.
- 17 Y. Negishi, W. Kurashige, Y. Niihori, T. Iwasa and K. Nobusada, *Phys. Chem. Chem. Phys.*, 2010, **12**, 6219-6225.
- 18 H. Qian, D.-e. Jiang, G. Li, C. Gayathri, A. Das, R. R. Gil and R. Jin, *J. Am. Chem. Soc.*, 2012, **134**, 16159-16162.
- 19 W. Kurashige, K. Munakata, K. Nobusada and Y. Negishi, *Chem Commun*, 2013, **49**, 5447-5449.
- 20 D. R. Kauffman, D. Alfonso, C. Matranga, H. Qian and R. Jin, *J. Phys. Chem. C*, 2013, **117**, 7914-7923.
- 21 X. Y. Dou, X. Yuan, Q. F. Yao, Z. T. Luo, K. Y. Zheng and J. P. Xie, *Chem Commun*, 2014, **50**, 7459-7462.
- 22 C. Kumara and A. Dass, *Nanoscale*, 2012, **4**, 4084-4086.
- 23 Y. Negishi, K. Igarashi, K. Munakata, W. Ohgake and K. Nobusada, *Chem Commun*, 2012, **48**, 660-662.
- 24 L. A. Porter, A. E. Ribbe and J. M. Buriak, *Nano Lett.*, 2003, **3**, 1043-1047.
- 25 J. Y. Chen, B. Wiley, J. McLellan, Y. J. Xiong, Z. Y. Li and Y. N. Xia, *Nano Lett.*, 2005, **5**, 2058-2062.
- 26 S. E. Skrabalak, L. Au, X. Li and Y. Xia, *Nat. Protoc.*, 2007, **2**, 2182-2190.
- 27 L. Au, X. Lu and Y. Xia, *Adv. Mater.*, 2008, **20**, 2517-2522.
- 28 Q. B. Zhang, J. P. Xie, J. Y. Lee, J. X. Zhang and C. Boothroyd, *Small*, 2008, **4**, 1067-1071.
- 29 M. Rycenga, C. M. Cobley, J. Zeng, W. Li, C. H. Moran, Q. Zhang, D. Qin and Y. Xia, *Chem. Rev.*, 2011, **111**, 3669-3712.
- 30 Y. Xia, W. Li, C. M. Cobley, J. Chen, X. Xia, Q. Zhang, M. Yang, E. C. Cho and P. K. Brown, *Acc. Chem. Res.*, 2011, **44**, 914-924.
- 31 K. W. Kim, S. M. Kim, S. Choi, J. Kim and I. S. Lee, *Acc. Chem. Res.*, 2012, **45**, 5122-5129.
- 32 W. Zhang, J. Yang and X. Lu, *Acc. Chem. Res.*, 2012, **45**, 7397-7405.
- 33 C. Zhu, S. Guo and S. Dong, *Adv. Mater.*, 2012, **24**, 2326-2331.
- 34 M. Liu, Y. Lu and W. Chen, *Adv. Funct. Mater.*, 2013, **23**, 1289-1296.
- 35 C. Wang, Y. Wang, L. Xu, X. Shi, X. Li, X. Xu, H. Sun, B. Yang and Q. Lin, *Small*, 2013, **9**, 413-420.
- 36 Z. Wu, *Angew. Chem., Int. Ed.*, 2012, **51**, 2934-2938.
- 37 X. W. Liu, D. S. Wang and Y. D. Li, *Nano Today*, 2012, **7**, 448-466.
- 38 G. L. Liu, D. Q. Feng, W. J. Zheng, T. F. Chen and D. Li, *Chem Commun*, 2013, **49**, 7941-7943.
- 39 J. Sun, H. X. Wu and Y. D. Jin, *Nanoscale*, 2014, **6**, 5449-5457.
- 40 M. Wang, Z. Wu, Z. Chu, J. Yang and C. Yao, *Chem. Asian. J.*, 2014, **9**, 1006-1010.
- 41 M. B. Li, S. K. Tian, Z. Wu and R. Jin, *Chem Commun*, 2015, **51**, 4433-6.
- 42 C. Yao, J. Chen, M.-B. Li, L. Liu, J. Yang and Z. Wu, *Nano Lett.*, 2015, **15**, 1281-1287.
- 43 A. Ghosh, J. Hassinen, P. Pulkkinen, H. Tenhu, R. H. Ras and T. Pradeep, *Anal Chem*, 2014, **86**, 12185-90.
- 44 M. Z. Zhu, W. T. Eckenhoff, T. Pintauer and R. C. Jin, *J Phys Chem C*, 2008, **112**, 14221-14224..
- 45 Z. Wu and R. Jin, *Nano Lett*, 2010, **10**, 2568-2573.
- 46 Z. Wu, J. Suhan and R. Jin, *J Mater Chem*, 2009, **19**, 622-626.

**TOC graphic:** Novel strategies to tune the compositions, structures and properties of nanoparticles were provided by varying ion-precursor and ion-dose in anti-galvanic reduction.

